Journal Pre-proofs

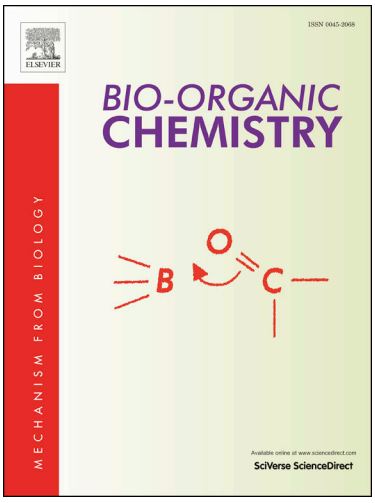

New 2,6,9-trisubstituted purine derivatives as Bcr-Abl and Btk inhibitors and as promising agents against leukemia

Jeanluc Bertrand, Hana Dostálová, Vladimír Kryštof, Radek Jorda, Alejandro Castro, Jaime Mella, Christian Espinosa-Bustos, Ana María Zarate, Cristian O. Salas

PII: S0045-2068(19)31549-4
DOI: https://doi.org/10.1016/j.bioorg.2019.103361
Reference: YBIOO 103361

To appear in: *Bioorganic Chemistry*

Received Date: 17 September 2019
Accepted Date: 12 October 2019

Please cite this article as: J. Bertrand, H. Dostálová, V. Kryštof, R. Jorda, A. Castro, J. Mella, C. Espinosa-Bustos, A. María Zarate, C.O. Salas, New 2,6,9-trisubstituted purine derivatives as Bcr-Abl and Btk inhibitors and as promising agents against leukemia, *Bioorganic Chemistry* (2019), doi: https://doi.org/10.1016/j.bioorg.2019.103361

New 2,6,9-trisubstituted purine derivatives as Bcr-Abl and Btk inhibitors and as promising agents against leukemia

Jeanluc Bertrand,[1] Hana Dostálová,[2] Vladimír Kryštof,[2,*] Radek Jorda,[2] Alejandro Castro,[3] Jaime Mella,[4] Christian Espinosa-Bustos,[5] Ana María Zarate,[1] and Cristian O. Salas[1,*]

[1] Departamento de Química Orgánica, Facultad de Química y de Farmacia, Pontificia Universidad Católica de Chile, 702843, Santiago de Chile, Chile.

[2] Laboratory of Growth Regulators, Palacký University and Institute of Experimental Botany, The Czech Academy of Sciences, Slechtitelu 27, 783 71 Olomouc, Czech Republic.

[3] Laboratorio de Bioproductos Farmacéuticos y Cosméticos, Centro de Excelencia en Medicina Traslacional, Facultad de Medicina, Universidad de La Frontera, Av. Francisco Salazar 01145, Temuco, 4780000, Chile

[4] Instituto de Química y Bioquímica, Facultad de Ciencias, Universidad de Valparaíso, 2360102, Av. Gran Bretaña 1111, Playa Ancha, Valparaíso, Casilla 5030, Chile.

[5] Departamento de Farmacia, Facultad de Química y de Farmacia, Pontificia Universidad Católica de Chile, 702843, Santiago de Chile, Chile.

Abstract

Bcr-Abl and Btk kinases are among the targets that have been considered for the treatment of leukemia. Therefore, several strategies have focused on the use of inhibitors as chemotherapeutic tools to treat these types of leukemia, such as imatinib (for Bcr-Abl) or ibrutinib (for Btk). However, the efficacy of these drugs has been reduced due to resistance mechanisms, which have motivated the development of new and more effective compounds. In this study, we designed, synthesized and evaluated 2,6,9-trisubstituted purine derivatives as novel Bcr-Abl and Btk inhibitors. We identified **5c** and **5d** as potent inhibitors of both kinases (IC_{50} values of 40 nM and 0.58/0.66 μM for Abl and Btk, respectively). From docking and QSAR analyses, we concluded that fluorination of the arylpiperazine system is detrimental to the activity against two kinases, and we also validated our hypothesis that the substitution on the 6-phenylamino ring is important for the inhibition of both kinases. In addition, our studies indicated that most compounds could suppress the proliferation of leukemia and lymphoma cells (HL60, MV4-11, CEM, K562 and Ramos cells) at low micromolar concentrations *in vitro*. Finally, we preliminarily demonstrated that **5c** inhibited the downstream signaling of both kinases in the respective cell models. Therefore, **5c** or **5d** possessed potency to be further optimized as anti-leukemia drugs by simultaneously inhibiting the Bcr-Abl and Btk kinases.

Graphical Abstract

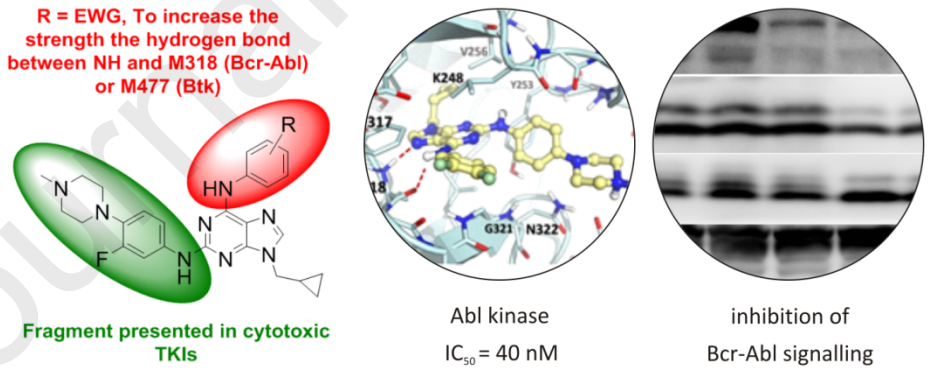

Keywords

Purine derivatives, Bcr-Abl inhibitors, Btk inhibitors, leukemia, docking, QSAR.

1. Introduction

Leukemia is a group of hematologic malignancies within a very large number of genetically diverse diseases, including an array of cancer types [1, 2] Today, numerous therapies exist to treat leukemia, such as the use of tyrosine kinase inhibitors (TKIs), which have been very successful.[3-5] The therapeutic potential of protein kinases has been widely accepted, and over 37 kinase inhibitor drugs have received approval for clinical use in certain cancers. [6] In fact, the kinase domain is the most common domain in known oncogenes. Mutations and other genetic aberrations often cause hyperactivation or changes in expression levels.[7] For example, the vast majority of chronic myelocytic leukemia (CML) cases and 20–30 % of acute lymphocytic leukemia (ALL) cases are caused by a reciprocal chromosomal translocation between chromosomes 9 and 22—t(9, 22)—thus forming the so-called Philadelphia chromosome (Ph).[8] This translocation results in the break-point cluster region-Abelson (*Bcr-Abl*) fusion gene, encoding a constitutively active protein tyrosine kinase, the Bcr-Abl fusion protein, which can deregulate tyrosine kinase activity. The dysregulated activity of Bcr-Abl is considered both a necessary and sufficient inducer of CML because it drives survival and proliferation through multiple downstream pathways.[9] Considering the role of Bcr-Abl in leukemia, in the 1980s, a therapeutic effort was directed towards the development of those specific inhibitors.[10, 11] Imatinib (**Figure 1**) was discovered as the first selective Bcr-Abl TKI, which elicited a high response rate and low toxicity, and the long-term survival of patients treated with imatinib currently makes it the frontline agent of choice for CML. Second-line treatments include dose escalation of imatinib and the second-generation TKIs dasatinib and nilotinib.[12] Despite the increase in overall survival promoted by imatinib,[13] more than 25 % of patients with CML will switch TKIs during their lifetime because of resistance or intolerance. Most resistance is due to amino acid substitutions in Bcr-Abl, mainly within the kinase domain.[14, 15] One of the most frequent mutations, ranging from 2 to 20 % of CML cases, is T315I (Ile replaces Thr at position 315 of Bcr-Abl), which is also the deadliest case since it leads to resistance to second-generation TKIs, such as nilotinib and dasatinib.[16, 17]

Another tyrosine kinase aberrantly activated in some hematological malignancies is Bruton's tyrosine kinase (Btk), which is a nonreceptor cytoplasmic protein tyrosine kinase usually expressed in immune cells such as B cells, mast cells and macrophages.[18, 19] The deregulation of Btk has been observed in mantle cell lymphoma (MCL), chronic lymphocytic leukemia (CLL), acute myelocytic leukemia (AML) and activated B-cell-diffuse large B-cell lymphoma. Btk is both a key regulator and a major kinase of the

B-cell receptor (BCR) signaling pathway and plays an important role in the regulation of B-cell activation, survival, proliferation and differentiation.[18] Thus, Btk mediates B-cell proliferation and apoptosis and can be considered a prospective target for the treatment of autoimmune diseases and cancer.[20, 21] In recent years, many small-molecule Btk inhibitors that bind to Btk catalytic domains have been reported.[4, 22] Ibrutinib (**Figure 1**) is an irreversible Btk inhibitor and has an acrylamide group in its structure, which can form a covalent bond by Michael addition with the conserved noncatalytic cysteine residue (C481) of Btk to achieve strong binding.[23] To capitalize on the efficacy of ibrutinib, several second-generation Btk inhibitors have been developed, such acalabrutinib, which has demonstrated significant activity in patients with CLL and MCL.[24] However, similar to imatinib, Btk inhibitors have also elicited resistance, limiting their clinical efficacy. This mechanism is associated with the C481M Btk mutation.[25, 26]

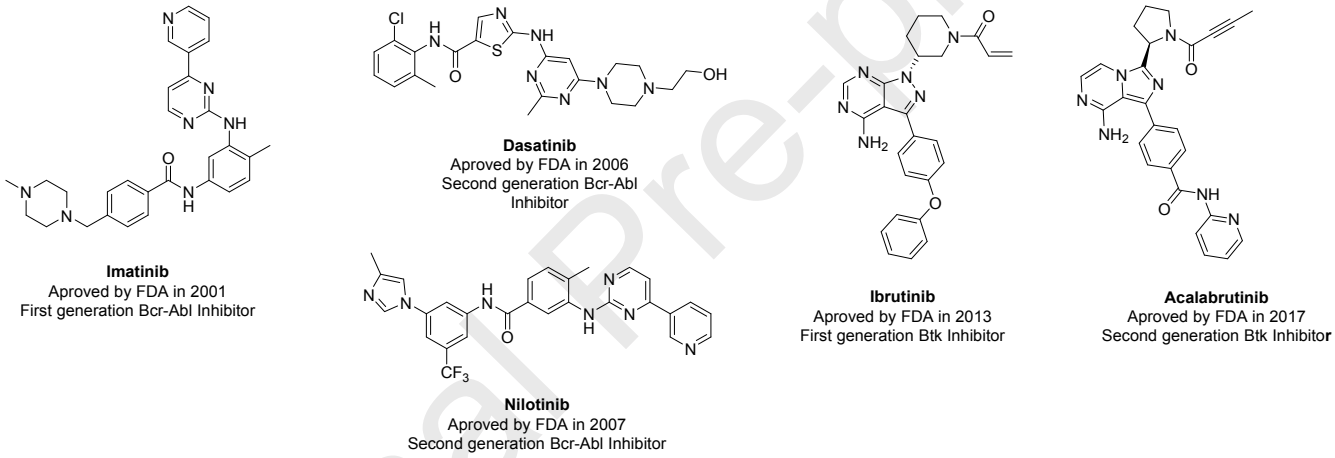

Figure 1. Chemical structures of some TKIs used in the treatment of leukemia.

Most of the Bcr-Abl and Btk inhibitors reported are heterocyclic compounds, and several of them are nitrogen heterocycles.[4, 10] These compounds share nitrogen heterocycle scaffolds as part of their structures (**Figure 1**), which in most cases is a pyrimidine ring. Therefore, in the search for new Bcr-Abl and Btk inhibitors, an extension of the pyrimidine system, such as the purine ring or isostere derivatives, has been studied.[27, 28] From these results, key information about the substitution patterns of the purine ring has been collected. For example, Wang et al.,[29], developed compound AP-23464 (**Figure 2**), which has a high affinity for Bcr-Abl. The aniline substitution on C-6 (together with the N7 atom) favored the interaction by hydrogen bonding with M321, and alkylation on N-7 favored the interaction with the hydrophobic pocket. Both of these interactions are important for the binding mode with Bcr-Abl.

Likewise, Qing Shi et al.,[30] optimized a heterocyclic fragment for new Btk inhibitors. Their results indicate that the purine core elicited the best performance on Btk (**Figure 2**, compound **I**). Once again, NH (from the aniline fragment) together with N7 favored the interaction by hydrogen bonding, in this case, with M477 in the Btk pocket. In addition, purvalanol B, a JAK3 inhibitor,[31] also elicited slight biochemical potency against Bcr-Abl. Crystallographic studies[32] demonstrated that this purine derivative had an interaction between the purine nitrogen (N7) and the N-H of M318 in the binding pocket (PDB:6BL8).

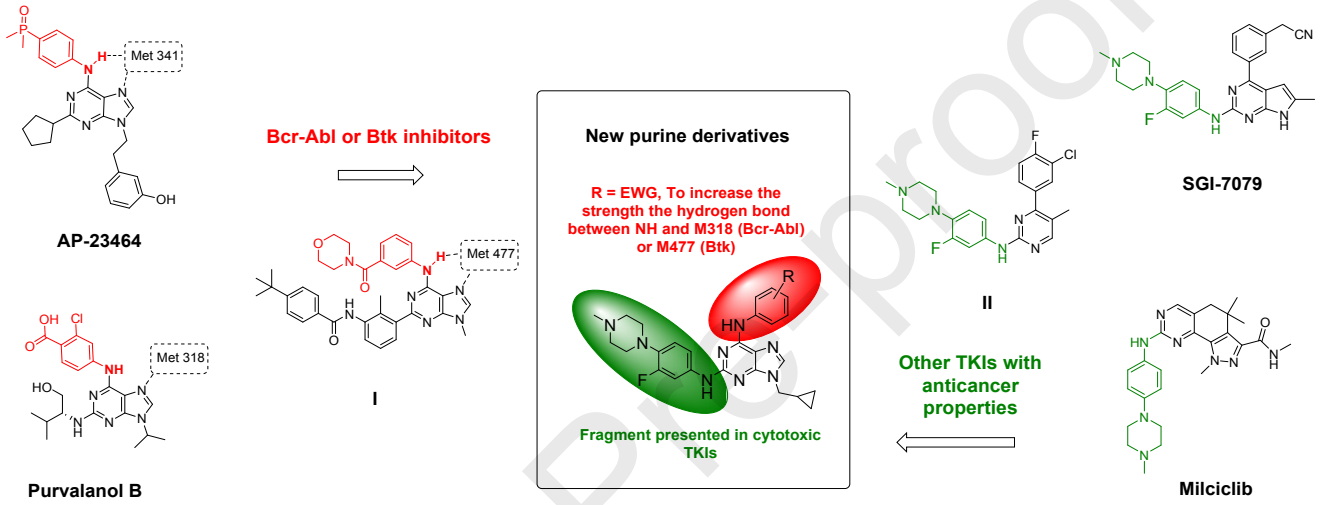

Figure 2. Chemical structures of 2,6,9-trisubstituted purines with biological properties and the design of the proposed compounds.

As mentioned, specific resistance often reduces the sensitivity of oncogenic kinases to drugs during therapy; therefore, novel molecules or approaches are intensively sought. In this work, during our programs to develop 2,6,9-trisubstituted purine derivatives with antitumor activity,[33] we report a new collection of 13 purine derivatives with interesting effects on Bcr-Abl and Btk activities. First, in the design of our compounds, the aniline fragment of the aforementioned kinase inhibitors (**Figure 2**, left side), was substituted with some electron-withdrawing groups (EWG), with the goal of increasing the strength of the hydrogen bond in both binding pockets. Second, considering that the chemical structures of some other kinase inhibitors that exhibit anticancer properties (including the CDK inhibitor milciclib[34] and the Axl inhibitors SGI-7079[35] and **II**[36] (**Figure 2**, right side), contains the *N*-methyl-piperazinyl-phenylamine moiety, we used this fragment in our compounds. In addition, the cytotoxic effect of these new purine derivatives on some cancer cell lines related to hematological

malignancies was assayed, and *in silico* studies were carried out to understand the structure-activity relationship on both kinases.

2. Results and discussions

2.1 Synthesis

We synthesized new 2,6,9-trisubstituted purines **5a-m** using short, simple and efficient synthetic methods, as described in **Scheme 1**.[33, 37, 38] We obtained fourteen compounds using 2,6-dichloropurine (**1**) as a starting material. The first step was the alkylation of **1** with the respective alkyl halides under basic conditions to give a mixture of *N-9-* and *N-7*-alkylated purine regioisomers **2a-a'** at a proportion of 4:1.[33] The second step was a regioselective nucleophilic substitution (S_NAr) at position C-6 with several anilines using *n*-butanol as the solvent, *N*,*N*-diisopropylethylamine as the base, at 110 ºC for 12 h to obtain high yields of compounds **3a-g**. Finally, a Buchwald-Hartwig coupling reaction at C-2 of **3a-g** with 4-(4-methylpiperazin-1-yl)aniline or 3-fluoro-4-(4-methylpiperazin-1-yl)aniline (**4a** or **4b**) promoted by MW and catalyzed by palladium (II) yielded the purine derivatives **5a-m** in moderate to high yields. **4a** and **4b** were previously synthesized from the respective fluoronitrobenzene compounds (**6a-b**). We purified all compounds by column chromatography and established their structures based on their spectral properties (IR, MS, ^{1}H NMR and ^{13}C NMR, see the experimental section and Supplementary Information, SI).

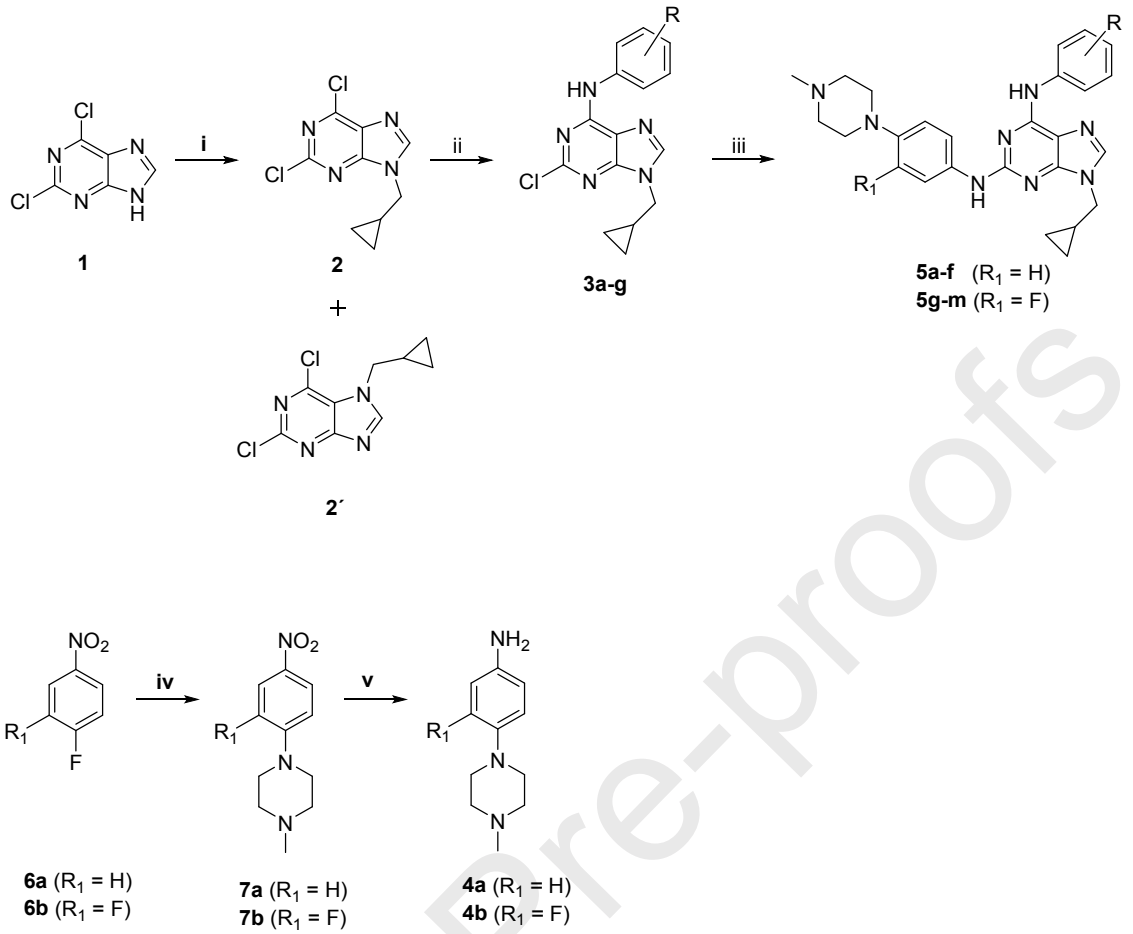

Scheme 1. *Reagents and conditions:* i) (Bromomethyl)cyclopropane, K_2CO_3, DMF, 12 h, RT. ii) Anilines, DIPEA, *n*-butanol, reflux, 12 h. iii) 4-(4-Methylpiperazin-1-yl)aniline **4a** or 3-fluoro-4-(4-methylpiperazin-1-yl)aniline **4b**, 2M K_2CO_3, $Pd(OAc)_2$, xantphos, dioxane, MW, 100 °C, 2 h. iv) *N*-Methylpiperazine, K_2CO_3, DMF, 2 h. v) Hydrazine, Pd-C, ethanol, 70 °C, 2 h.

2.2. Kinase inhibition

Due to the known inhibitory effect of related 6-anilino purines on tyrosine kinases,[39] we screened all prepared compounds for inhibitory activity against Abl and Btk. As expected, the Abl kinase was the most sensitive kinase to inhibition by several compounds at submicromolar concentrations; the most active compounds, **5c** and **5d**, displayed IC_{50} values of 40 nM (**Table 1**). The latter compound was also most active against the Btk kinase, with an IC_{50} of 0.58 μM. The serine/threonine kinase Cdk-2 was assayed in parallel and was approximately two orders of magnitude less sensitive, confirming selectivity towards tyrosine kinases.

Our observation suggests that fluorination of the *N*-methyl-piperazinyl-phenylamine at purine position 2 is detrimental for activity against Abl; its presence reduces inhibitory activity by approximately ten-fold (e.g., **5a** vs **5g**, **5b** vs **5h**, **5c** vs **5i**, **5d** vs **5j** and **5f** vs **5m**). We also found that the substitution on the 6-phenylamino ring markedly influenced the inhibitory potency in both directions, depending both on its type and position. For example, with respect to **5a** or **5g** (without substitution on the aniline ring), the presence of fluorine in *meta* slightly increased or maintained the potency towards Abl (**5b** or **5i**, respectively), whereas *para*-fluorine substitution (**5b**, **5h**) reduced the potency. Interestingly, the comparison of the pair **5b** and **5d** or **5h** and **5i** indicated that the positive effect of *meta*-fluorine was stronger than the negative effect of *para*-fluorine, difluorine derivatives. However, when disubstitution was performed with fluorine at the *meta/para* position on the 6-phenylamino ring, the increased potency of **5d** and **5j** towards Abl was similar to the reference compound. Likewise, a methoxy group in the *para* position slightly increased the potency towards Abl (**5k**). We also noted that a combination of chlorine with one or two methoxy groups lead to a decrease in potency (**5e**, **5f**, **5l** and **5m**). Similar but much weaker effects of this substitution were also observed on Btk inhibition.

Table 1. *In vitro* inhibition of compounds **5a-m** on the kinases Abl, Btk and Cdk-2/Cyclin E.

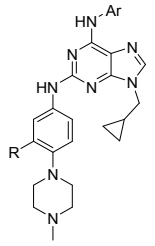

Compound	Ar	R	IC_{50} (μM)[a] Abl	Btk	Cdk-2/Cyclin E
5a		H	0.09 ± 0.01	0.90 ± 0.18	21.64 ± 3.80
5b		H	0.11 ± 0.01	1.30 ± 0.29	11.03 ± 1.83
5c		H	0.04 ± 0.01	0.66 ± 016	24.00 ± 6.00
5d		H	0.04 ± 0.01	0.58 ± 0.19	18.49 ± 6.76
5e	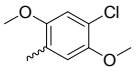	H	36.00 ± 3.86	>100	28.61 ± 6.23
5f	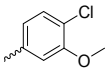	H	0.80 ± 0.07	21.68 ± 9.66	16.80 ± 3.12
5g		F	0.58 ± 0.10	2.01 ± 0.60	14.93 ± 1.88
5h		F	1.07 ± 0.24	3.46 ± 0.94	9.01 ± 2.96
5i		F	0.60 ± 0.07	1. 81 ± 0.46	22.10 ± 4.75
5j	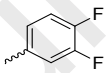	F	0.58 ± 0.05	2.65 ± 0.02	13. 73 ± 3.54
5k	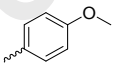	F	0.34 ± 0.06	3.17 ± 0.00	10.90 ± 1.97
5l	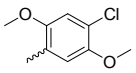	F	>100	>100	29.42 ± 6.80
5m	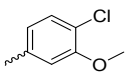	F	8.43 ± 1.27	>100	22.18 ± 4.82

[a] IC_{50} values were determined in at least three independent experiments in the range of 0.01-100 μM.

2.3 Quantitative structure-activity relationship (QSAR)

From the results shown in **Table 1** and to propose a rational series of structural modifications that give rise to a new family of compounds, we carried out analyses of quantitative structure-activity relationships (QSARs) to guide the synthesis of the new molecules. We found an equation for Bcr-Abl (**Eq. 1**) and one for Btk (**Eq. 2**). In Tables S1 and S2, we report the experimental versus predicted activity for each equation (Bcr-Abl and Btk, respectively). Figures S1 and S2 show the regression graph for each equation (supplementary material).

$$pIC_{50} = 355.46 - 65.55CMR_B - 1.072Clpara_A - 1.630MeOortho_A \quad \textbf{(Eq. 1)}$$

$$r^2 = 0.9742; MS = 0.0259; F = 100.73; p = 1 * 10^{-6}$$

$$pIC_{50} = 9.065 - 1.426piB + 0.201FmetaA - 1.322ClparaA \quad \textbf{(Eq. 2)}$$

$$r^2 = 0.9527; MS = 0.597; F = 40.29; p = 0.000227$$

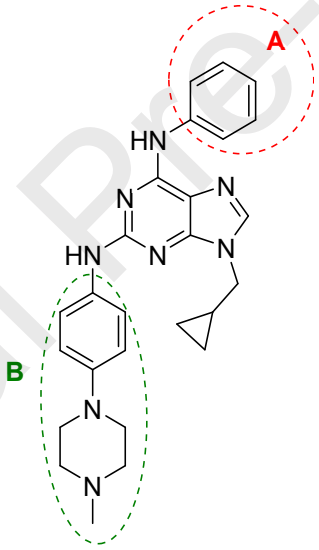

The analysis of equation 1 for Bcr-Abl showed that:

i. Abl inhibition is inversely proportional to the molar refractivity of fragment B (CMR B). This means that the insertion of high refractivity groups in this portion of the molecule is not favorable (e.g., Cl, Br or I).

ii. It is not favorable to insert a chlorine atom in a *para* position on ring A (Cl*para* A). Additionally, the insertion of a methoxy group in the *ortho* position on ring A (MeO*ortho* A) is not favorable. Therefore, the addition of these functional groups to these positions should be avoided. The *meta* position of the ring could be explored more freely.

The analysis of equation 2 for Btk shows us that:

i. Btk inhibition decreases as the lipophilicity of the "B" ring system increases. Therefore, it is not favorable to increase lipophilicity in this region. Preferably, substitutions that reduce lipophilicity and that do not prevent the protonation of the piperazine system should be inserted.

ii. Activity towards Btk is increased by the presence of a fluorine atom in the A-ring (F*meta*A). Considering both this information and the previously obtained Abl equation, an insertion at the *meta* position would probably generate the most bioactive compounds.

iii. The activity is drastically reduced if chlorine atoms are inserted in *para* position at ring A (Cl*para*A). The insertion of groups with electronic properties other than chlorine at this position or that reduce the size of the group is encouraged. The most active compounds have no substitutions at the *para* position on ring A or have a fluorine atom.

2.4 Docking studies

With the goal of rationalizing the inhibition of Abl and Btk and the differences in the inhibition of both kinases by these purine derivatives, we carried out docking studies. From Abl and Btk analysis, the lowest energy **5d**-kinase complexes are shown in **Figure 4** (see SI for the values of all compounds in both kinases), using the respective reported crystal structures (Bcr-Abl, PDB code: 2GQG[40] and Btk, PDB code: 4OT5[41]). As we expected, the interactions that stabilized both complexes involved the same parts of the ligands, a hydrogen bond between the NH/N7 (purine moiety) and NH/CO (M318 or M477 residue). In addition, the interactions between the NH^+-piperazine ring and the respective residue (salt bridge for Abl and hydrogen bond for Btk) contributed to the stabilization of these complexes. In addition, compound **5d** established interactions of the π-π type between the difluorophenyl portion and the amino acids F317 and Y320 at the binding site of the Abl. This fact could explain the higher potency of **5d** towards Abl (IC_{50} = 40 nM) than towards Btk (IC_{50} = 0.58 μM), since in latter kinase, the aromatic portion would not establish a similar interaction. However, an interesting result is shown on the right side of **Figure 4**. In both cases, the position of the ligand was away from some amino acids that have been reported as point of molecular mutations related to resistance to imatinib (T315) or ibrutinib (C481).

a)

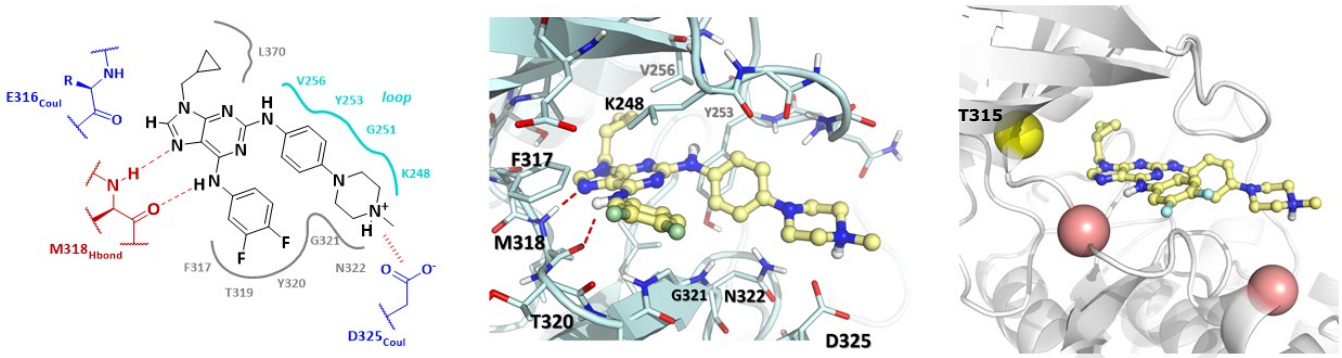

b)

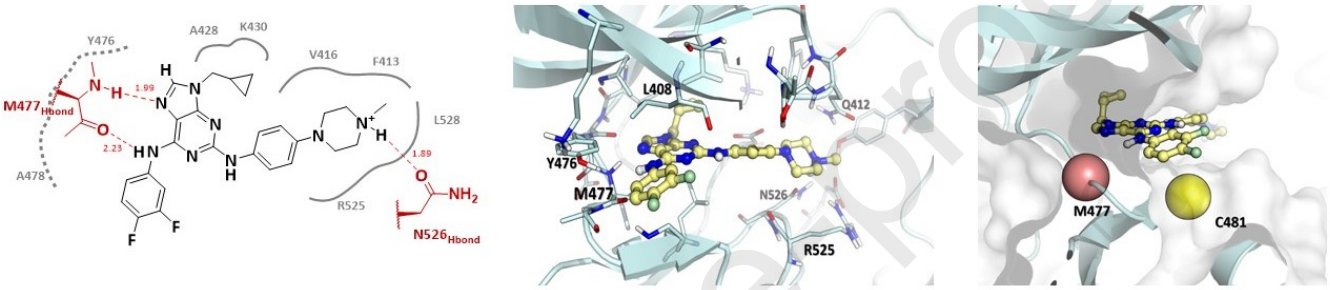

Figure 4. Different views of the molecular docking modes of **5d** at the binding site: **a)** for Abl and **b)** for Btk. *On the left-side*, 2D representations show the main interactions in the binding pocket; *in the middle*, 3D view; and *on the right-side,* a representation of **5d** with the amino acids that are observed in the mutant forms of these kinases.

The compounds that showed low activity (**5e**, **5l** and **5m**) against both kinases contain bulky functional groups in the phenyl ring linked to position 6 of the purine. This structure causes steric limitations, which increase the distance between the NH fragment and the N7 of the purine derivatives to form hydrogen bonds with M318 or M477 in Abl and Btk, respectively (see supplementary information).

2.5 Cytotoxic studies

We screened all prepared compounds for cytotoxic activity against the cancer cell lines HL-60 (acute promyelocytic leukemia), MV4-11 (acute myelogenous leukemia), CEM (acute lymphoblastic leukemia), K562 (chronic myelogenous leukemia), Ramos (non-Hodgkin lymphoma) and MCF7 (breast adenocarcinoma). All cell lines yielded micromolar GI_{50} values (**Table 2**). MV4-11 was the most sensitive cell line, and CEM was the least sensitive. Overall, compounds **5c** and **5d** were the most cytotoxic among the series of compounds with single digit micromolar GI_{50} values in all cell lines. In

general, the cytotoxicity of the prepared compounds was consistent with enhanced Abl inhibition, especially in the K562 cell line, with similar structure-activity relationships to those described above.

Table 2. *In vitro* cytotoxicity of compounds **5a-m** on cancer cell lines.

Compound	GI_{50} (μM)[a]					
	HL-60	**MV4-11**	**CEM**	**K562**	**Ramos**	**MCF-7**
5a	3.65 ± 0.76	1.72 ± 0.02	12.58 ± 0.56	1.53 ± 0.04	9.60 ± 0.65	6.84 ± 0.99
5b	3.06 ± 0.03	1.46 ± 0.18	10.65 ± 2.09	1.71 ± 0.00	7.56 ± 0.34	5.17 ± 0.37
5c	1.23 ± 0.20	1.65 ± 0.23	8.89 ± 0.18	0.77 ± 0.06	5.77 ± 0.32	4.17 ± 0.13
5d	1.17 ± 0.47	1.67 ± 0.19	7.62 ± 0.80	1.24 ± 0.27	4.63 ± 0.59	3.41 ± 0.42
5e	0.38 ± 0.05	4.38 ± 0.37	7.14 ± 0.71	4.70 ± 0.23	4.72 ± 0.15	9.03 ± 0.61
5f	0.71 ± 0.03	2.74 ± 0.67	6.89 ± 0.15	2.95 ± 0.01	4.53 ± 0.41	8.71 ± 0.54
5g	2.49 ± 0.52	1.35 ± 0.02	7.78 ± 0.02	3.61 ± 0.79	5.17 ± 0.88	4.95 ± 0.56
5h	1.60 ± 0.26	1.44 ± 0.16	8.00 ± 0.60	3.50 ± 0.16	4.73 ± 0.36	4.64 ± 0.20
5i	1.48 ± 0.05	1.37 ±0.13	5.98 ± 0.03	2.89 ± 0.21	4.33 ± 0.48	3.90 ± 0.06
5j	1.29 ± 0.17	1.48 ± 0.11	7.27 ± 0.61	2.17 ± 0.12	4.10 ± 0.37	4.12 ± 0.02
5k	1.39 ± 0.18	1.39 ± 0.11	8.20 ± 1.21	3.14 ± 0.86	7.24 ± 0.49	6.04 ± 0.14
5l	0.54 ± 0.01	4.09 ± 0.40	7.10 ± 0.24	4.55 ± 0.19	5.01 ± 0.27	9.25 ± 0.02
5m	0.68 ± 0.31	3.37 ± 0.39	7.38 ± 1.05	4.27 ± 0.30	3.91 ± 0.08	7.26 ± 1.81

[a] IC_{50} values were determined in three independent experiments in the range 0.1 to 25 μM, depending of the compound solubility.

Next, we wanted to demonstrate that **5c**, a representative of the most potent compounds, is able to inhibit Abl and Btk in cells. We therefore analyzed signaling pathways downstream of these kinases in cultured cells treated with various doses of **5c** for 1 h. In K562 cells, western blotting revealed decreased levels of phosphorylated Stat5 and CrkL, which are both well-established substrates of Bcr-Abl (**Figure 5a**). Btk inhibition was detected in Ramos cells, in which the Btk signaling pathway requires activation by immunoglobulin M. Cells exposed to **5c** responded by reducing the level of phospho-Btk (Y223) in a dose-dependent manner as a result of blocked autophosphorylation, and by decreasing the phosphorylation of its downstream targets, the kinases Erk1/2 and Akt and phospholipase PLCγ2, which together confirms the efficient suppression of the pathway (**Figure 5b**).

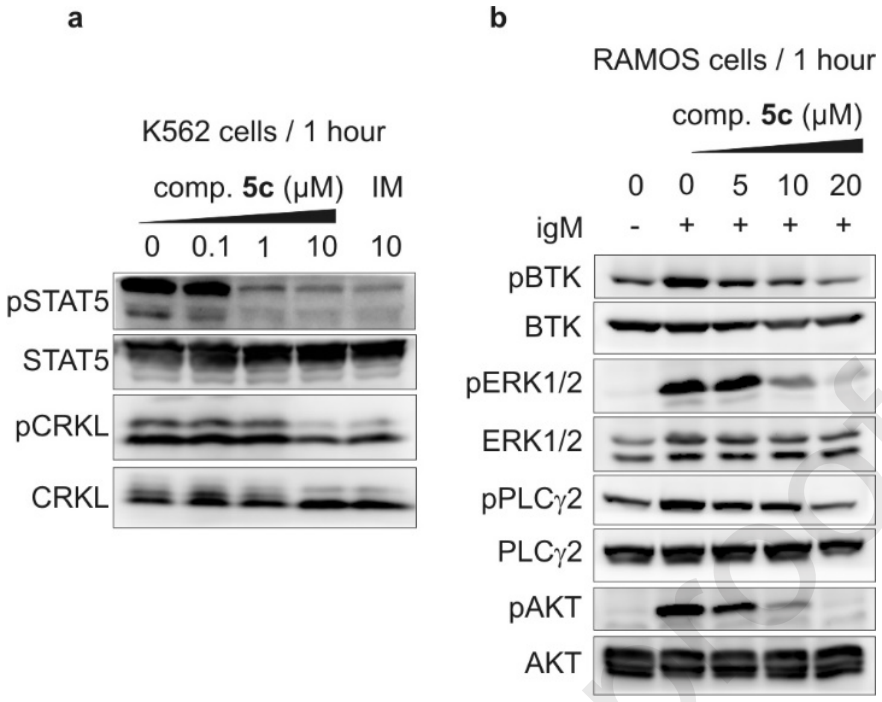

Figure 5. Compound **5c** inhibits Bcr-Abl and Btk activity in cells. **a)** K562 cells were treated with vehicle or the indicated concentration of **5c** for 1 h; imatinib (IM, 10 μM) was used as a positive control. **b)** Ramos cells were treated with vehicle or the indicated dose of **5c** for 1 h and stimulated with anti-IgM (5 μg/ml) for 10 minutes before harvesting. Cells were lysed, and proteins were detected by immunoblotting.

3. Conclusions

This study on the effect of new 2,6,9-trisubstituted purines on two tyrosine kinases involved in leukemia, Bcr-Abl and Btk, showed that certain chemical modifications of the aniline moiety increased the inhibitory activity against both proteins. Two of these compounds, **5c** and **5d**, were highly potent and exhibited cytotoxicity against six cancer cell lines. Our results confirm a previous conclusion that the purine core is a privilege scaffold to develop new Bcr-Abl/Btk inhibitors, and structure-activity relationships indicated that the substitution of a fluorine atom on the aniline fragment at *meta*- or *para*-positions enhanced the activity towards Abl and Btk. However, fluorination of the *N*-methyl-piperazinyl-phenylamine moiety decreased the potency of both kinases. The docking studies identified the main interactions of inhibitors with Abl and Btk and helped to show the difference in potency against both kinases. Likewise, **5c** was able to inhibit Abl and Btk in cells, which was demonstrated by monitoring some kinases that are in the downstream signaling pathways of both kinases. These results showed that the **5c** and **5d** compounds are simpler than the TKIs in clinical trials and, according to our results, could be considered promising leads for the development of new anti-leukemia drugs.

4. Experimental

4.1 Materials and measurements

Melting points were determined on a Kofler Thermogerate apparatus and were uncorrected. Infrared spectra were recorded on a JASCO FT/IR-400 spectrophotometer. Nuclear magnetic resonance spectra were recorded, unless otherwise specified, on a Bruker AM-400 instrument using deuterated chloroform or dimethylsulfoxide solutions containing tetramethylsilane as an internal standard. Mass spectra were obtained on an HP 5988A mass spectrometer. HRMS-ESI-MS experiments were performed using a Thermo Scientific Exactive Plus Orbitrap spectrometer with a constant nebulizer temperature of 250 °C. The experiments were carried out in positive or negative ion mode, with a scan range of m/z 300.00-1510.40 with a resolution of 140 000. The samples were infused directly into the ESI source via a syringe pump at flow rates of 5 $\mu L \cdot min^{-1}$ through the instrument's injection valve. Thin layer chromatography (TLC) was performed using Merck GF-254 type 60 silica gel. Column chromatography was carried out using Merck type 9385 silica gel. The purity of the compounds was determined by TLC and high-resolution mass spectrometry (HRMS).

4.2 Synthesis

To a solution of 2,6-dichloro-9*H*-purine (**1**, 2.0 g, 1.058 mol), (bromomethyl)cyclopropane (2.14 g, 1.58 mol) and K_2CO_3 (3.36 mg, 3.174 mol) in DMF (20 mL) were added, and the mixture was stirred at room temperature for 12 h. The mixture was filtrated and evaporated. The residue was purified by silica gel chromatography using a polarity mobile phase (acetone/dichloromethane, 5:100) to give products **2** and **2´**.

2,6-Dichloro-9-(cyclopropylmethyl)-9*H*-purine, (2)

White solid, yield 51 %, mp 88-89 °C. ^{1}H NMR (400 MHz, $CDCl_3$) δ 8.22 (s, 1H), 4.10 (d, J = 7.4 Hz, 2H), 1.33 (ddd, J = 12.4, 7.8, 4.8 Hz, 1H), 0.72 (q, J = 5.6 Hz, 2H), 0.48 (q, J = 5.2 Hz, 2H). ^{13}C NMR (101 MHz, $CDCl_3$) δ 153.31, 153.02, 151.81, 145.52, 130.88, 77.16, 49.48, 11.03, 4.64 ppm. ESI/MS for ($C_9H_8Cl_2N_4$ $[M+H]^+$). Calcd: 243.0. Found: 242.9.

2,6-Dichloro-7-(cyclopropylmethyl)-7*H*-purine, (2´)

White solid, yield 18 %, mp 90-91 °C. ^{1}H NMR (400 MHz, $CDCl_3$) δ 8.40 (s, 1H), 4.33 (d, J = 7.3 Hz, 2H), 1.47 – 1.31 (m, 1H), 0.85 – 0.66 (m, 2H), 0.48 (q, J = 5.1 Hz, 2H). ^{13}C NMR (101 MHz, $CDCl_3$) δ 163.63, 153.01, 149.90, 143.77, 121.80, 52.50, 11.56, 4.67. ESI/MS for ($C_9H_8Cl_2N_4$ [M+H]+). Calcd: 243.0. Found: 242.9.

*General procedures for the synthesis compounds **3a-g***

To a solution of **2** (100 mg, 0.411 mmol), aniline (154 mg, 0.411 mmol) and DIPEA (0.15 mL, 0.822 mmol) in *n*-butanol (20 mL) were added, and the mixture was stirred at 110 °C for 12 h. After cooling to room temperature, the reaction mixture was concentrated. The residue was purified by silica gel chromatography using a polarity mobile phase (acetone/dichloromethane, 10:100) to give product **3a**.

2-Chloro-9-(cyclopropylmethyl)-*N*-phenyl-9*H*-purin-6-amine (3a) White solid, yield 85 %, mp 158-160 °C. ^{1}H NMR (400 MHz, $CDCl_3$) δ 8.11 (s, 1H, N-H), 7.89 (s, 1H), 7.78 (d, *J* = 8.2 Hz, 2H), 7.38 (t, *J* = 7.7 Hz, 2H), 7.13 (t, *J* = 7.2 Hz, 1H), 4.02 (d, *J* = 7.3 Hz, 2H), 1.39 – 1.24 (m, 1H), 0.68 (q, *J* = 5.4 Hz, 2H), 0.45 (q, *J* = 5.2 Hz, 2H). ^{13}C NMR (101 MHz, $CDCl_3$) δ 154.18, 152.46, 150.85, 140.56, 138.27, 129.22, 124.10, 120.38, 119.25, 48.78, 11.17, 4.49 ppm. ESI/MS for ($C_{15}H_{14}ClN_5$ $[M+H]^+$). Calcd: 300.1. Found: 299.7.

2-Chloro-9-(cyclopropylmethyl)-*N*-(4-fluorophenyl)-9*H*-purin-6-amine (3b) White solid, yield 89 %, mp 143-144 °C. ^{1}H NMR (400 MHz, $CDCl_3$) δ 8.22 (s, 1H, N-H), 7.87 (s, 1H), 7.71 (dd, *J* = 8.9, 4.7 Hz, 2H), 7.06 (t, *J* = 8.6 Hz, 2H), 4.02 (d, *J* = 7.3 Hz, 2H), 1.40 – 1.20 (m, 1H), 0.68 (q, *J* = 5.5 Hz, 2H), 0.44 (q, *J* = 5.1 Hz, 2H). ^{13}C NMR (101 MHz, $CDCl_3$) δ 160.51, 158.09, 154.06, 152.33, 150.75, 140.51, 134.15, 134.12, 122.21, 122.14, 118.96, 115.84, 115.61, 48.68, 11.04, 4.36. ^{19}F NMR (376 MHz, $CDCl_3$) δ -118.39 (s, 1F) ppm. ESI/MS for ($C_{15}H_{13}ClFN_5$ $[M+H]^+$). Calcd: 318.1. Found: 317.8.

2-Chloro-9-(cyclopropylmethyl)-*N*-(3-fluorophenyl)-9*H*-purin-6-amine (3c) White solid, yield 76 %, mp 140-142 °C.^{1}H NMR (400 MHz, $CDCl_3$) δ 8.21 (s, 1H, N-H), 7.92 (s, 1H), 7.79 (d, *J* = 11.1 Hz, 1H), 7.41 (d, *J* = 8.2 Hz, 1H), 7.31 (dd, *J* = 14.8, 8.0 Hz, 1H), 6.81 (td, *J* = 8.3, 2.2 Hz, 1H), 4.04 (d, *J* = 7.3 Hz, 2H), 1.32 (qd, *J* = 7.6, 3.7 Hz, 1H), 0.69 (q, *J* = 5.4 Hz, 2H), 0.46 (q, *J* = 5.2 Hz, 2H). ^{13}C NMR (101 MHz, $CDCl_3$) δ 164.28, 161.85, 153.95, 152.04, 150.88, 140.71, 139.83, 139.72, 130.18, 130.08, 119.18, 115.39, 115.36, 110.59, 110.38, 107.63, 107.36, 48.73, 11.04, 4.38. ^{19}F NMR (376 MHz, $CDCl_3$) δ -111.18 (s, 1F) ppm. ESI/MS for ($C_{15}H_{13}ClFN_5$ $[M+H]^+$). Calcd: 318.1. Found: 317.8.

2-Chloro-9-(cyclopropylmethyl)-*N*-(3,4-difluorophenyl)-9*H*-purin-6-amine (3d) White solid, yield 77 %, mp 138-139 °C. ^{1}H NMR (400 MHz, $CDCl_3$) δ 8.04 (s, 1H, N-H), 7.91 (s, 1H), 7.90 – 7.84 (m, 1H), 7.35 – 7.28 (m, 1H), 7.14 (q, *J* = 9.2 Hz, 1H), 4.04 (d, *J* = 7.3 Hz, 2H), 1.39 – 1.24 (m, 1H), 0.69 (q, *J* = 5.4 Hz, 2H), 0.45 (q, *J* = 5.2 Hz, 2H). ^{13}C NMR (101 MHz, $CDCl_3$) δ 154.05, 152.11, 151.54, 151.41, 151.06, 149.09, 148.95, 148.22, 148.10, 145.79, 145.66, 140.99, 134.85, 134.82, 134.76, 134.73, 119.23, 117.51, 117.34, 116.02, 115.98, 115.96, 115.93, 110.18, 109.96, 77.16, 48.88, 11.17, 4.51. ^{19}F NMR (376 MHz, $CDCl_3$) δ -135.31 (d, *J* = 21.8 Hz), -143.20 (d, *J* = 21.8 Hz) ppm. ESI/MS for ($C_{15}H_{12}ClF_2N_5$ $[M+H]^+$). Calcd: 336.1. Found: 336.0.

2-Chloro-9-(cyclopropylmethyl)-*N*-(4-methoxyphenyl)-9*H*-purin-6-amine (3e) White solid, yield 81 %, mp 183-185 °C. ^{1}H NMR (400 MHz, $CDCl_3$) δ 8.02 (s, 1H, N-H), 7.84 (s, 1H), 7.62 (d, *J* = 8.9 Hz, 2H), 6.91 (t, *J* = 6.1 Hz, 2H), 4.00 (d, *J* = 7.3 Hz, 2H), 3.81 (s, 3H), 1.37 – 1.23 (m, 1H), 0.66 (q, *J* = 5.4 Hz, 2H), 0.43 (q, *J* = 5.2 Hz, 2H). ^{13}C NMR (101 MHz, $CDCl_3$) δ 156.58, 154.28, 152.70, 150.74, 140.45, 131.15, 122.58, 119.06, 114.39, 77.16, 55.63, 48.70, 11.18, 4.45 ppm. ESI/MS for ($C_{16}H_{16}ClN_5O$ $[M+H]^+$). Calcd: 330.1. Found: 329.7.

2-Chloro-*N*-(4-chloro-2,5-dimethoxyphenyl)-9-(cyclopropylmethyl)-9*H*-purin-6-amine (3f) White solid, yield 62 %, mp 148-151 °C.^{1}H NMR (400 MHz, DMSO) δ 8.42 (s, 1H, N-H), 8.32 (s, 1H), 8.20 (s, 1H), 6.99 (s, 1H), 4.00 (d, *J* = 7.3 Hz, 2H), 3.85 (s, 3H), 3.83 (s, 3H), 1.36 – 1.23 (m, 1H), 0.58 – 0.52 (m, 2H), 0.43 (q, *J* = 5.0 Hz, 2H). ^{13}C NMR (101 MHz, DMSO) δ 152.17, 151.29, 150.42, 148.17, 141.97, 126.59, 118.90, 114.65, 112.36, 105.76, 56.37, 56.00, 47.78, 39.52, 10.93, 3.74 ppm. ESI/MS for ($C_{17}H_{17}Cl_2N_5O_2$ $[M+H]^+$). Calcd: 394.1. Found: 394.0.

2-Chloro-*N*-(4-chloro-3-methoxyphenyl)-9-(cyclopropylmethyl)-9*H*-purin-6-amine (3g) White solid, yield 76 %, mp 216-218 °C. ^{1}H NMR (400 MHz, $CDCl_3$) δ 8.14 (s, 1H, N-H), 7.87 (s, 1H), 7.86 (d, *J* = 2.1 Hz, 1H), 3.99 (d, *J* = 7.3 Hz, 2H), 3.92 (s, 3H), 1.28 (ddd, *J* = 12.4, 7.8, 4.8 Hz, 1H), 0.65 (q, *J* = 5.5 Hz, 2H), 0.42 (q, *J* = 5.2 Hz, 2H). ^{13}C NMR (101 MHz, $CDCl_3$) δ 155.30, 153.90, 152.07, 150.93, 140.78, 138.24, 130.09, 119.26, 116.92, 112.38, 104.78, 77.16, 56.23, 48.85, 11.14, 4.50 ppm. ESI/MS for ($C_{16}H_{15}Cl_2N_5O$ $[M+H]^+$). Calcd: 364.1. Found: 363.9.

*General procedures for the synthesis compounds **7a-b***

To a solution of **6a** (1000 mg, 7.1 mmol), 1-methylpiperazine (708 mg, 7.1 mmol) and K_2CO_3 (2226 mg, 21 mmol) in DMF (20 mL) were added, and the mixture was stirred at room temperature for 2 h. Then, the reaction mixture was poured into 400 mL of cold water and filtered, and the solid was dried in the oven at 80 °C for 2 h to give product **7a**. The same procedure was used for compound **7b**.

1-Methyl-4-(4-nitrophenyl)piperazine (7a)

Orange solid, yield 98 %, mp 105-107 °C. ^{1}H NMR (400 MHz, $CDCl_3$) δ 8.09 (d, *J* = 9.4 Hz, 2H), 6.80 (d, *J* = 9.4 Hz, 2H), 3.48 – 3.37 (m, 4H), 2.58 – 2.50 (m, 4H), 2.35 (s, 3H). ^{13}C NMR (101 MHz, $CDCl_3$) δ 154.91, 138.55, 126.03, 112.79, 77.16, 54.59, 47.02, 46.10. ESI/MS for ($C_{11}H_{15}N_3O_2$ $[M+H]^+$). Calcd: 222.1. Found: 221.4.

1-(2-Fluoro-4-nitrophenyl)-4-methylpiperazine (7b)

Red solid, yield 95 %, mp 98-100 °C. ^{1}H NMR (400 MHz, $CDCl_3$) δ 7.93 (dd, *J* = 8.9, 1.7 Hz, 1H), 7.85 (dd, *J* = 13.2, 2.4 Hz, 1H), 6.87 (t, J = 8.8 Hz, 1H), 3.35 – 3.19 (m, 4H), 2.66 – 2.45 (m, 4H), 2.32 (s,

3H). ^{13}C NMR (101 MHz, $CDCl_3$) δ 154.35, 151.87, 145.72, 145.65, 121.12, 121.09, 117.23, 117.19, 112.79, 112.53, 77.16, 54.85, 49.64, 49.59, 46.15. ^{19}F NMR (188 MHz, $CDCl_3$) δ -126.45. ESI/MS for ($C_{11}H_{14}FN_3O_2$ $[M+H]^+$). Calcd: 240.1. Found: 240.3.

*General procedures for the synthesis compounds **4a-b***

To a solution of **7a** (300 mg, 1.35 mmol), Pd-C (30 mg) in ethanol (20 mL) was added, and the mixture was stirred under reflux for 1 h. Then, hydrazine (2.6 mL) was added dropwise to the mixture and stirred over reflux for an additional 2 h. After the completion of the reaction, the reaction mixture was filtered in Celite and concentrated to give **4a**.

4-(4-Methylpiperazin-1-yl)aniline (4a)

Black solid, yield 99 %, mp 128-130 °C. ^{1}H NMR (400 MHz, $CDCl_3$) δ 6.80 (t, J = 9.1 Hz, 1H), 6.48 – 6.33 (m, 2H), 3.53 (s, 2H), 3.10 – 2.83 (m, 4H), 2.66 – 2.54 (m, 4H), 2.34 (s, 3H). ^{13}C NMR (101 MHz, $CDCl_3$) δ 144.55, 140.23, 118.67, 116.29, 77.16, 55.39, 50.89, 46.17. ESI/MS for ($C_{11}H_{17}N_3$ $[M+H]^+$). Calcd: 192.2. Found: 191.9.

3-Fluoro-4-(4-methylpiperazin-1-yl)aniline (4b)

Black solid, yield 98 %, mp 120-125 °C. ^{1}H NMR (400 MHz, $CDCl_3$) δ 6.80 (t, J = 9.1 Hz, 1H), 6.48 – 6.33 (m, 2H), 3.53 (s, 2H), 3.10 – 2.83 (m, 4H), 2.66 – 2.54 (m, 4H), 2.34 (s, 3H). ^{13}C NMR (101 MHz, $CDCl_3$) δ 159.14, 154.27, 142.94, 142.73, 131.59, 131.39, 120.56, 120.47, 110.65, 110.59, 104.06, 103.59, 55.13, 50.81, 50.77, 45.73. ^{19}F NMR (376 MHz, $CDCl_3$) δ -122.56 (s, 1F). ESI/MS for ($C_{11}H_{16}FN_3$ $[M+H]^+$). Calcd: 210.1. Found: 210.3.

*General procedures for the synthesis of final compounds **5a-m***

To a solution of **3a** (150 mg, 0.519 mmol) and **4a** (110 mg, 0.57 mmol) or **4b** (120 mg, 0.57 mmol) in dioxane (2 mL), $Pd(OAc)_2$ (24 mg, 0.1 mmol), xantphos (120 mg, 0.2 mmol) and 2 M K_2CO_3 (aq) (1 mL, 0.2 mmol) were added, and the mixture was stirred at 100 °C for 1 h in a microwave reactor. After cooling to room temperature, the reaction mixture was filtrated in celite, and the filtrate was diluted with H_2O (100 mL). The mixture was extracted with EtOAc, and the organic layer was dried by anhydrous Na_2SO_4 and concentrated. The residue was purified by silica gel chromatography using a polarity mobile phase (methanol/dichloromethane, 10:100) to give a final product.

9-(Cyclopropylmethyl)-*N*^{2}-(4-(4-methylpiperazin-1-yl)phenyl)-*N*^{6}-phenyl-9*H*-purine-2,6-diamine (5a) White solid, yield 60 %, mp 88-89 °C. ^{1}H NMR (400 MHz, $CDCl_3$) δ 8.08 (s, 1H), 7.68 (d, J = 8.1 Hz, 2H), 7.61 (s, 1H), 7.50 (d, J = 8.9 Hz, 2H), 7.23 (t, J = 7.8 Hz, 2H), 7.19 (s, 1H), 6.99 (t, J = 7.3 Hz,

1H), 6.87 (d, *J* = 8.9 Hz, 2H), 3.84 (d, *J* = 7.2 Hz, 2H), 3.17 – 3.07 (m, 4H), 2.61 – 2.50 (m, 4H), 2.31 (s, 3H), 1.22 (qd, *J* = 7.4, 2.5 Hz, 1H), 0.58 (q, *J* = 5.4 Hz, 2H), 0.36 (q, *J* = 5.1 Hz, 2H). ^{13}C NMR (101 MHz, $CDCl_3$) δ 156.84, 152.21, 151.27, 146.68, 139.18, 137.78, 133.41, 128.74 (2C), 122.94, 120.91 (2C), 120.36 (2C), 116.97 (2C), 115.21, 55.19 (2C), 50.03, 48.07 (2C), 46.11, 11.04, 4.28 (2C) ppm. ESI/MS for ($C_{26}H_{30}N_8$ $[M+H]^+$). Calcd: 455.2666. Found: 455.2671.

9-(Cyclopropylmethyl)-*N*^{6}-(4-fluorophenyl)-*N*^{2}-(4-(4-methylpiperazin-1-yl)phenyl)-9*H*-purine-2,6-diamine (5b) White solid, yield 52 %, mp 148-149 °C. ^{1}H NMR (400 MHz, $CDCl_3$) δ 8.11 (s, 1H), 7.91 (t, *J* = 6.7 Hz, 3H), 7.76 (d, *J* = 8.7 Hz, 2H), 7.23 (t, *J* = 8.7 Hz, 2H), 7.20 (s, 1H), 7.16 (d, *J* = 8.8 Hz, 2H), 4.17 (d, *J* = 7.1 Hz, 2H), 3.47 – 3.38 (m, 4H), 2.90 – 2.77 (m, 4H), 2.60 (s, 3H), 1.54 (ddd, *J* = 15.3, 10.2, 6.1 Hz, 1H), 0.90 (q, *J* = 5.3 Hz, 2H), 0.68 (q, *J* = 5.1 Hz, 2H). ^{13}C NMR (101 MHz, $CDCl_3$) δ 159.97, 157.57, 156.78, 152.13, 151.31, 146.79, 137.79, 135.11, 135.08, 133.22, 122.05, 121.97 (2C), 120.92 (2C), 116.94 (2C), 115.46 (2C), 115.24, 115.07, 55.20 (2C), 50.00 (2C), 48.12, 46.11, 11.07, 4.29. ^{19}F NMR (376 MHz, $CDCl_3$) δ -119.90 (s, 1F) ppm. ESI/MS for ($C_{26}H_{29}FN_8$ $[M+H]^+$). Calcd: 473.2572. Found: 473.2571.

9-(Cyclopropylmethyl)-*N*^{6}-(3-fluorophenyl)-*N*^{2}-(4-(4-methylpiperazin-1-yl)phenyl)-9*H*-purine-2,6-diamine (5c) White solid, yield 45 %, mp 79-81 °C. ^{1}H NMR (400 MHz, $CDCl_3$) δ 8.28 (s, 1H), 8.15 (d, *J* = 11.6 Hz, 1H), 7.95 (s, 1H), 7.80 (d, *J* = 8.7 Hz, 2H), 7.54 – 7.43 (m, 2H), 7.27 (s, 1H), 7.22 (d, *J* = 8.7 Hz, 2H), 6.99 (t, *J* = 7.7 Hz, 1H), 4.20 (d, *J* = 7.2 Hz, 2H), 3.52 – 3.40 (m, 4H), 2.95 – 2.83 (m, 4H), 2.63 (s, 3H), 1.61 – 1.53 (m, 1H), 0.93 (q, *J* = 5.3 Hz, 2H), 0.71 (q, *J* = 5.1 Hz, 2H). ^{13}C NMR (101 MHz, $CDCl_3$) δ 164.28, 161.86, 156.86, 151.84, 151.44, 147.01, 140.87, 140.75, 137.94, 132.95, 129.77, 129.67, 121.32 (2C), 117.04(2C), 115.26, 115.05, 115.03, 109.39, 109.18, 107.45, 107.18, 55.21(2C), 49.95(2C), 48.14, 46.13, 11.05, 4.29. ^{19}F NMR (376 MHz, $CDCl_3$) δ -111.75 (s, 1F) ppm. ESI/MS for ($C_{26}H_{29}FN_8$ $[M+H]^+$). Calcd: 473.2572. Found: 473.2578.

9-(Cyclopropylmethyl)-*N*^{6}-(3,4-difluorophenyl)-*N*^{2}-(4-(4-methylpiperazin-1-yl)phenyl)-9*H*-purine-2,6-diamine (5d) White solid, yield 61 %, mp 125-126 °C. ^{1}H NMR (400 MHz, $CDCl_3$) δ 8.09 (s, 1H), 7.97 (ddd, *J* = 12.8, 7.3, 2.5 Hz, 1H), 7.68 (s, 1H), 7.51 (d, *J* = 8.8 Hz, 2H), 7.13 (d, *J* = 8.9 Hz, 1H), 7.08 (s, 1H), 7.02 (dd, *J* = 18.5, 9.1 Hz, 1H), 6.95 (d, *J* = 8.9 Hz, 2H), 3.92 (d, *J* = 7.2 Hz, 2H), 3.26 – 3.11 (m, 4H), 2.68 – 2.53 (m, 4H), 2.36 (s, 3H), 1.30 (ddd, *J* = 10.2, 7.5, 3.7 Hz, 1H), 0.66 (q, *J* = 5.4 Hz, 2H), 0.44 (q, *J* = 5.1 Hz, 2H). ^{13}C NMR (101 MHz, $CDCl_3$) δ 156.88, 151.75, 151.47, 151.24, 151.11, 148.67, 147.09, 144.89, 144.76, 137.99, 135.87, 135.78, 132.85, 121.41 (2C), 116.97 (2C), 116.73, 115.27, 115.06, 109.71, 109.49, 55.20 (2C), 49.90 (2C), 48.14, 46.12, 11.03, 4.29. ^{19}F NMR (376 MHz,

$CDCl_3$) δ -136.18 (d, *J* = 22.1 Hz, 1F), -145.05 (d, *J* = 22.1 Hz, 1F) ppm. ESI/MS for ($C_{26}H_{28}F_2N_8$ [M+H]+). Calcd: 491,2478. Found: 491.2482.

N6-(4-chloro-2,5-dimethoxyphenyl)-9-(cyclopropylmethyl)-N2-(4-(4-methylpiperazin-1-yl)phenyl)-9H-purine-2,6-diamine (5e) White solid, yield 38 %, mp 103-104 °C. ^{1}H NMR (400 MHz, CDCl3) δ 8.18 (s, 1H), 7.81 (s, 1H), 7.47 (s, 1H), 7.24 (d, *J* = 8.8 Hz, 2H), 6.73 (s, 1H), 6.66 (d, *J* = 8.9 Hz, 2H), 6.63 (s, 1H), 3.68 (d, *J* = 7.1 Hz, 2H), 3.61 (s, 3H), 3.38 (s, 3H), 3.03 – 2.83 (m, 4H), 2.46 – 2.36 (m, 4H), 2.15 (s, 3H), 1.16 – 0.94 (m, 1H), 0.41 (q, *J* = 5.4 Hz, 2H), 0.26 – 0.10 (m, 2H). ^{13}C NMR (101 MHz, CDCl3) δ 156.67, 151.69, 151.33, 148.95, 146.87, 142.67, 138.14, 133.11, 128.03, 121.47 (2C), 120.79, 117.15, 117.00 (2C), 115.84, 114.32, 111.97, 105.90, 56.98, 56.35, 55.06, 49.68, 48.04, 45.91, 11.08, 4.25 ppm. ESI/MS for ($C_{28}H_{33}ClN_8O_2$ [M+H]+). Calcd: 549.2488. Found: 549.2490.

***N*^{6}-(4-chloro-3-methoxyphenyl)-9-(cyclopropylmethyl)-*N*^{2}-(4-(4-methylpiperazin-1-yl)phenyl)-9*H*-purine-2,6-diamine (5f)** White solid, yield 42 %, mp 96-98 °C. ^{1}H NMR (400 MHz, $CDCl_3$) δ 7.99 (s, 1H), 7.70 (s, 1H), 7.51 (d, *J* = 8.8 Hz, 2H), 7.42 (s, 1H), 7.23 (s, 2H), 7.04 (s, 1H), 6.92 (d, *J* = 8.9 Hz, 2H), 3.93 (d, *J* = 7.2 Hz, 2H), 3.72 (s, 3H), 3.25 – 3.13 (m, 4H), 2.66 – 2.58 (m, 4H), 2.38 (s, 3H), 1.39 – 1.23 (m, 1H), 0.67 (q, *J* = 5.4 Hz, 2H), 0.45 (q, *J* = 5.1 Hz, 2H). ^{13}C NMR (101 MHz, $CDCl_3$) δ 156.76, 155.02, 151.96, 151.44, 146.94, 138.94, 138.00, 133.04, 129.84, 121.20 (2C), 116.93 (2C), 116.08, 115.29, 112.88, 104.80, 56.06, 55.17, 49.90, 48.13, 46.09, 11.06, 4.29 ppm. ESI/MS for ($C_{27}H_{31}ClN_8O$ [M+H]$^+$). Calcd: 519.2382. Found: 519.2386.

9-(Cyclopropylmethyl)-*N*^{2}-(3-fluoro-4-(4-methylpiperazin-1-yl)phenyl)-*N*^{6}-phenyl-9*H*-purine-2,6-diamine (5g) White solid, yield 61 %, mp 93-94 °C. ^{1}H NMR (400 MHz, $CDCl_3$) δ 7.69 (s, 1H), 7.66 – 7.62 (m, 1H), 7.61 (d, *J* = 5.5 Hz, 3H), 7.23 (t, *J* = 7.9 Hz, 2H), 7.03 – 6.99 (m, 1H), 6.97 (d, *J* = 4.1 Hz, 2H), 6.80 (t, *J* = 9.1 Hz, 1H), 3.84 (d, *J* = 7.2 Hz, 2H), 2.99 (s, 4H), 2.52 (s, 4H), 2.26 (s, 3H), 1.29 – 1.15 (m, 1H), 0.56 (q, *J* = 5.6 Hz, 2H), 0.35 (q, *J* = 5.1 Hz, 2H). ^{13}C NMR (101 MHz, $CDCl_3$) δ 156.98, 156.11, 154.56, 152.24, 151.06, 138.81, 138.11, 136.01, 135.90, 134.39, 134.29, 128.91, 123.33, 120.49, 119.11, 119.07, 115.57, 114.51, 114.48, 108.03, 107.77, 55.28, 50.95, 50.93, 48.22, 46.13, 11.08, 4.31. ^{19}F NMR (376 MHz, $CDCl_3$) δ -121.75 (s, 1F) ppm. ESI/MS for ($C_{26}H_{29}FN_8$ [M+H]$^+$). Calcd: 473.2572. Found: 473.2578.

9-(Cyclopropylmethyl)-*N*^{2}-(3-fluoro-4-(4-methylpiperazin-1-yl)phenyl)-*N*^{6}-(4-fluorophenyl)-9*H*-purine-2,6-diamine (5h) White solid, yield 63 %, mp 96-103 °C. ^{1}H NMR (400 MHz, $CDCl_3$) δ 8.43 (s, 1H), 7.96 (d, *J* = 17.6 Hz, 2H), 7.87 (dd, *J* = 8.3, 4.8 Hz, 2H), 7.55 (s, 1H), 7.32 (d, *J* = 8.2 Hz, 1H), 7.23 (t, *J* = 8.5 Hz, 2H), 7.13 (t, *J* = 9.1 Hz, 1H), 4.18 (d, *J* = 7.1 Hz, 2H), 3.33 (s, 4H), 2.87 (s, 4H), 2.61 (s, 3H), 1.61 – 1.51 (m, 1H), 0.91 (q, *J* = 5.1 Hz, 2H), 0.68 (t, *J* = 4.9 Hz, 2H). ^{13}C NMR (101 MHz, $CDCl_3$)

δ 160.15, 157.74, 156.92, 156.14, 154.49, 152.26, 151.08, 138.09, 135.99, 135.88, 134.86, 134.83, 134.36, 134.27, 122.49 (2C), 122.41, 119.06, 119.02, 115.50 (2C), 115.28, 115.25, 114.47, 114.44, 108.00, 107.74, 55.23 (2C), 50.91 (2C), 50.89, 48.20, 46.10, 11.03, 4.29. ^{19}F NMR (376 MHz, $CDCl_3$) δ -119.37 (s, 1F), -121.69 (s, 1F) ppm. ESI/MS for ($C_{26}H_{28}F_2N_8$ $[M+H]^+$). Calcd: 491.2478. Found: 491.2484.

9-(Cyclopropylmethyl)-*N*^{2}-(3-fluoro-4-(4-methylpiperazin-1-yl)phenyl)-*N*^{6}-(3-fluorophenyl)-9*H*-purine-2,6-diamine (5i) White solid, yield 55 %, mp 93-95 °C. ^{1}H NMR (400 MHz, $CDCl_3$) δ 8.07 (s, 1H), 7.63 (d, *J* = 11.4 Hz, 1H), 7.57 (s, 1H), 7.52 (dd, *J* = 14.8, 2.3 Hz, 1H), 7.23 (s, 1H), 7.11 – 6.99 (m, 3H), 6.77 (t, *J* = 9.1 Hz, 1H), 6.58 (dd, *J* = 10.4, 5.0 Hz, 1H), 3.79 (d, *J* = 7.2 Hz, 2H), 2.96 (s, 4H), 2.48 (s, 4H), 2.22 (s, 3H), 1.20 – 1.09 (m, 1H), 0.52 (q, *J* = 5.5 Hz, 2H), 0.30 (q, *J* = 5.0 Hz, 2H). ^{13}C NMR (101 MHz, $CDCl_3$) δ 164.20, 161.78, 156.92, 156.13, 154.49, 151.91, 151.23, 140.66, 140.55, 138.31, 135.78, 135.68, 134.59, 134.49, 129.81, 129.71, 119.16, 119.12, 115.52, 115.38, 115.35, 114.93, 114.90, 109.63, 109.41, 108.25, 108.00, 107.62, 107.35, 55.25 (2C), 50.87, 50.84 (2C), 48.24, 46.11, 11.01, 4.31. ^{19}F NMR (376 MHz, $CDCl_3$) δ -111.86 (s, 1F), -121.72 (s, 1F) ppm. ESI/MS for ($C_{26}H_{28}F_2N_8$ $[M+H]^+$). Calcd: 491.2478. Found: 491.2481.

9-(Cyclopropylmethyl)-*N*^{6}-(3,4-difluorophenyl)-*N*^{2}-(3-fluoro-4-(4-methylpiperazin-1-yl)phenyl)-9*H*-purine-2,6-diamine (5j) White solid, yield 68 %, mp 94-97 °C. ^{1}H NMR (400 MHz, $CDCl_3$) δ 8.08 (s, 1H), 7.87 (ddd, *J* = 12.6, 7.2, 2.5 Hz, 1H), 7.71 (s, 1H), 7.65 (dd, *J* = 14.8, 2.4 Hz, 1H), 7.23 (s, 1H), 7.15 (dd, *J* = 7.4, 5.3 Hz, 2H), 7.04 (dd, *J* = 18.5, 9.1 Hz, 1H), 6.92 (t, *J* = 9.1 Hz, 1H), 3.95 (d, *J* = 7.2 Hz, 2H), 3.09 (s, 4H), 2.62 (s, 4H), 2.36 (s, 3H), 1.34 – 1.27 (m, 1H), 0.70 – 0.62 (m, 2H), 0.45 (q, *J* = 5.0 Hz, 2H). ^{13}C NMR (101 MHz, $CDCl_3$) δ 156.91, 156.11, 154.48, 151.84, 151.25, 151.13, 148.82, 148.69, 147.52, 147.39, 145.09, 144.97, 138.32, 135.63, 135.52, 134.90, 134.73, 134.63, 119.15, 119.11, 117.05, 116.87, 115.70, 115.67, 115.35, 114.95, 109.93, 109.71, 108.32, 108.17, 108.07, 55.26 (2C), 53.43, 50.88 (2C), 50.85, 48.27, 46.12, 31.57, 22.64, 14.10, 11.03, 4.31. ^{19}F NMR (376 MHz, $CDCl_3$) δ -121.65 (s, 1F), -136.18 (d, J = 22.0 Hz, 1F), -144.55 (d, J = 22.0 Hz, 1F) ppm. ESI/MS for ($C_{26}H_{27}F_3N_8$ $[M+H]^+$). Calcd: 509.2384. Found: 509.2390.

9-(Cyclopropylmethyl)-*N*^{2}-(3-fluoro-4-(4-methylpiperazin-1-yl)phenyl)-*N*^{6}-(4-methoxyphenyl)-9*H*-purine-2,6-diamine (5k) White solid, yield 55 %, mp 85-86 °C. ^{1}H NMR (400 MHz, $CDCl_3$) δ 8.03 (s, 1H), 7.75 (dd, *J* = 15.0, 2.3 Hz, 1H), 7.68 (s, 1H), 7.58 (d, *J* = 8.9 Hz, 2H), 7.23 (s, 1H), 7.08 (dd, *J* = 8.6, 2.1 Hz, 1H), 6.88 (dt, *J* = 9.4, 4.6 Hz, 3H), 3.94 (d, *J* = 7.2 Hz, 2H), 3.80 (s, 3H), 3.09 (s, 4H), 2.64 (s, 4H), 2.37 (s, 3H), 1.30 (dd, *J* = 10.2, 5.1 Hz, 1H), 0.66 (q, *J* = 5.5 Hz, 2H), 0.44 (q, *J* = 5.1 Hz, 2H). ^{13}C NMR (101 MHz, $CDCl_3$) δ 156.97, 156.18, 156.04, 154.54, 152.57, 150.90, 137.86, 136.25, 136.14,

134.08, 133.99, 131.81, 122.86 (2C), 119.11, 119.07, 115.23, 114.23 (2C), 114.20, 114.09, 107.77, 107.51, 55.51, 55.23 (2C), 50.89, 50.86 (2C), 48.16, 46.06, 31.57, 22.64, 14.11, 11.05, 4.28. ^{19}F NMR (376 MHz, $CDCl_3$) δ -121.55 (s, 1F) ppm. ESI/MS for ($C_{27}H_{31}FN_8O$ $[M+H]^+$). Calcd: 503.2678. Found: 503.2677.

***N*^{6}-(4-chloro-2,5-dimethoxyphenyl)-9-(cyclopropylmethyl)-*N*^{2}-(3-fluoro-4-(4-methylpiperazin-1-yl)phenyl)-9*H*-purine-2,6-diamine (5l)** White solid, yield 40 %, mp 97-98 °C. ^{1}H NMR (400 MHz, $CDCl_3$) δ 8.35 (s, 1H), 8.00 (s, 1H), 7.70 (s, 1H), 7.55 (dd, *J* = 14.6, 2.3 Hz, 1H), 7.13 (dd, *J* = 8.6, 2.1 Hz, 1H), 6.87 (dd, *J* = 10.9, 4.7 Hz, 3H), 3.92 (d, *J* = 7.2 Hz, 2H), 3.83 (s, 3H), 3.71 (s, 3H), 3.14 – 3.02 (m, 4H), 2.63 (s, 4H), 2.36 (s, 3H), 1.28 (dd, *J* = 9.9, 5.2 Hz, 1H), 0.64 (q, *J* = 5.4 Hz, 2H), 0.42 (q, *J* = 5.2 Hz, 2H). ^{13}C NMR (101 MHz, $CDCl_3$) δ 156.91, 155.88, 154.48, 151.74, 151.08, 148.94, 142.88, 138.42, 135.82, 135.72, 134.54, 134.45, 127.79, 119.23, 119.19, 116.17, 114.98, 114.95, 114.78, 112.13, 108.27, 108.02, 106.03, 57.03, 56.37, 55.17 (2C), 50.69 (2C), 48.22, 45.97, 11.11, 4.29. ^{19}F NMR (376 MHz, $CDCl_3$) δ -121.55 (s, 1F) ppm. ESI/MS for ($C_{28}H_{32}ClFN_8O_2$ $[M+H]^+$). Calcd: 567.2394. Found:567.2396.

***N*^{6}-(4-chloro-3-methoxyphenyl)-9-(cyclopropylmethyl)-*N*^{2}-(3-fluoro-4-(4-methylpiperazin-1-yl)phenyl)-9*H*-purine-2,6-diamine (5m)** White solid, yield 60 %, mp 100-101 °C. ^{1}H NMR (400 MHz, $CDCl_3$) δ 8.44 (s, 1H), 7.79 (s, 1H), 7.74 (d, *J* = 14.8 Hz, 1H), 7.62 (d, *J* = 4.5 Hz, 1H), 7.36 (d, *J* = 8.5 Hz, 1H), 7.24 (dd, *J* = 17.5, 9.1 Hz, 3H), 6.96 (t, *J* = 9.1 Hz, 1H), 4.01 (d, *J* = 7.1 Hz, 2H), 3.78 (s, 3H), 3.18 (s, 4H), 2.71 (s, 4H), 2.45 (s, 3H), 1.36 (dd, *J* = 7.3, 4.9 Hz, 1H), 0.75 (d, *J* = 7.5 Hz, 2H), 0.53 (d, *J* = 4.5 Hz, 2H). ^{13}C NMR (101 MHz, $CDCl_3$) δ 156.87, 156.09, 154.89, 154.44, 152.01, 151.16, 138.72, 138.22, 135.89, 135.79, 134.47, 134.37, 129.77, 119.09, 119.05, 116.29, 115.40, 114.71, 114.68, 113.30, 108.10, 107.84, 104.93, 55.92, 55.21 (2C), 50.86, 50.83 (2C), 48.22, 46.08, 11.01, 4.31. ^{19}F NMR (376 MHz, $CDCl_3$) δ -121.59 (s, 1F) ppm. ESI/MS for ($C_{27}H_{30}ClFN_8O$ $[M+H]^+$). Calcd: 537.2288. Found: 537.2292.

4.3 Kinase assays

Abl1 and Cdk-2/cyclin E kinases were produced in-house, and Btk was purchased from ProQinase. The kinase reactions were assayed with a suitable substrate (500 µM peptide GGEAIYAAPFKK for Abl, 1 mg/mL histone H1 for CDK2, 100 µM poly(Glu:Tyr; 4:1)) in the presence of ATP (1 µM for Abl, 15 µM for Cdk-2 and Btk), 0.05 µCi [γ-^{33}P]ATP, and the test compound in a final volume of 10 µL of reaction buffer (60 mM HEPES-NaOH, pH 7.5, 3 mM $MgCl_2$, 3 mM $MnCl_2$, 3 µM Na-orthovanadate, 1.2 mM DTT, 2.5 µg/50 µL $PEG_{20.000}$). The reactions were stopped by adding 5 µL of 3 % aq. H_3PO_4.

Aliquots were spotted onto P-81 phosphocellulose (Whatman), washed 3× with 0.5 % aq. H_3PO_4 and finally air-dried. Kinase inhibition was quantified using a FLA-7000 digital image analyzer. The concentration of the test compounds required to reduce the activity by 50 % was determined from dose-response curves and reported as the IC_{50} value.

4.4 2D-QSAR

For the 2D-QSAR study, the molar refractivity (CMR) and lipophilicity (CLogP) parameters were calculated using ChemBioDraw software (15.1.0, PerkinElmer, Waltham, MA, USA). The multilinear regression analysis was performed with Statistica software (8.0, StatSoft, Tulsa, OK, USA). The biological activity was converted to a logarithmic scale ($pIC_{50} = -LogIC_{50}$) and was used as a dependent variable. ClogP, $ClogP^2$, CMR, and CMR^2 were used as independent variables for both the whole molecule and its fragments. Free-Wilson descriptors (X_i) for the presence ($X_i = 1$) or absence ($X_i = 0$) of -F, -Cl and $-OCH_3$ on the different rings were also considered (20 independent variables). All combinations among the independent variables with biological activity were evaluated. For the sequential search of combinations, the "best subsets" option was used in the "General Regression Models" menu of Statistica. The best model presented here contained the fewest number of independent variables to avoid overfitting,[42] and chance correlation[43] and to obtain the highest correlation coefficient.

4.5 Docking

The 3D structures of compounds synthetized were built using OECHEM followed by protonation states were adjusted to pH 7.2 using FixpKa from the QUACPAC package. The conformers were generated using OMEGA software. The crystalline structures of enzymes (Abl and Btk) were downloaded from the RCSB PDB Protein Data Bank (2GQG[40] and 4OT5[41], respectively). All water, ions and cofactors were removed. Next, hydrogen atoms and protons were added, and partial charges (in accordance with the protonation state at the physiological pH) were assigned. The preparation of the proteins was performed using the Chimera USCF program.[44] This was followed by a local minimization to relieve potential bad contacts. The minimization was performed in the presence of restraints to maintain the protein conformation very similar to that observed in the experimental model. The molecular docking studies were carried out by the FRED program, and docking runs were performed using the fast-rigid exhaustive docking approach implemented in the software.[45] In this case, the ChemGauss4 scoring function was used to evaluate and score the resulting docked poses. Next, the best poses were optimized using SZYBKI, and the energy of binding was estimated by taking into account the solvation energies of

the interacting molecules, in addition to the molecular mechanics (MM) energies. The contribution of polar solvation energies was computed by the generalized Born (GB) implicit solvent model, while the nonpolar contribution of the solvation energy was dependent on the solvent accessible surface area (SA).[46] The interactions of residues in the active site were identified using a 6 Å radius around the docked position as a reference. The pictures were obtained with PyMol software.

4.6 Cell Cultures

Human cell lines were obtained from the German Collection of Microorganisms and Cell Cultures and were cultivated according to the provider's instructions. MV4-11 cells were maintained in RPMI-1640 medium supplemented with 10 % fetal bovine serum, penicillin (100 U/mL), and streptomycin (100 µg/mL). CCRF-CEM cells were maintained in RPMI-1640 medium supplemented with 20 % fetal bovine serum, penicillin (100 U/mL), and streptomycin (100 µg/mL). The cell lines K562 and MCF-7 were cultivated in DMEM supplemented with 10 % fetal bovine serum, penicillin (100 U/mL), and streptomycin (100 µg/ml). Ramos cells (obtained from DSMZ) were maintained in IMDM supplemented with 10 % fetal bovine serum, penicillin (100 U/mL), and streptomycin (100 µg/mL). All cell lines were kept at 37 °C in 5 % CO_2. BTK activation in cells was induced by treatment with goat $F(ab')_2$ anti-human IgM purchased from Southern Biotech.

4.7 Cytotoxicity Assays

Cytotoxicity assays were performed using resazurin, an indicator dye to measure oxidation-reduction reactions occurring in the mitochondria of live cells. The cells were treated in triplicate with six different doses of each compound for 72 h. After treatment, a resazurin (Sigma Aldrich) solution was added for 4 h, and the fluorescence of resorufin corresponding to live cell quantity was measured at 544 nm/590 nm (excitation/emission) using a Fluoroskan Ascent microplate reader (Labsystems). The GI_{50} value, the drug concentration lethal to 50 % of the cells, was calculated from the dose response curves.

4.8 Immunoblotting

Cell lysates were separated on SDS-polyacrylamide gels and electroblotted onto nitrocellulose membranes. After blocking, overnight incubation with specific primary antibodies, and incubation with peroxidase-conjugated secondary antibodies, peroxidase activity was detected with SuperSignal West Pico reagents (Thermo Scientific) using a CCD camera LAS-4000 (Fujifilm). The following specific antibodies (Cell Signaling) were used: anti-BTK (#3533), anti-phospho-BTK Y223 (#5082),

anti-ERK1/2 (#9101), anti-phospho-ERK1/2 T202/Y204 (#9102), anti-AKT (#4691), anti-phospho-AKT S473 (#4060), anti-PLCγ2 (#3872), anti-phospho-PLCγ2 Y1217 (#3871), anti-STAT5 (#94205), anti-phospho-STAT5 Y694 (#9351), anti-Crkl (#3182), and anti-phospho-Crkl Y207 (#3181). Anti-PCNA (clone PC-10) was generously gifted by Dr. B. Vojtěšek.

Acknowledgments

The authors wish to acknowledge the support from FONDECYT (COS, Research Grant N° 1161816), the Ministry of Health of the Czech Republic (17-31834A), Palacký University in Olomouc (IGA_PrF_2019_013) and the European Regional Development Fund (Project ENOCH, No. CZ.02.1.01/0.0/0.0/16_019/0000868). JLB is grateful to CONICYT for a PhD fellowship (N° 21180975).

Notes and references

[1] G. Prakash, A. Kaur, P. Malhotra, A. Khadwal, P. Sharma, V. Suri, N. Varma, S. Varma, Current Role of Genetics in Hematologic Malignancies, Indian J. Hematol. Blood. Transfus, 32 (2016) 18-31.

[2] L.A. Godley, A. Shimamura, Genetic predisposition to hematologic malignancies: management and surveillance, Blood, 130 (2017) 424-432.

[3] F. Rossari, F. Minutolo, E. Orciuolo, Oncology, Past, present, and future of Bcr-Abl inhibitors: from chemical development to clinical efficacy, J. Hematol. Oncol. 11 (2018) 84.

[4] C. Liang, D. Tian, X. Ren, S. Ding, M. Jia, M. Xin, S. Thareja, The development of Bruton's tyrosine kinase (BTK) inhibitors from 2012 to 2017: A mini-review, Eur. J. Med. Chem. 151 (2018) 315-326.

[5] R. Kannaiyan, D. Mahadevan, A comprehensive review of protein kinase inhibitors for cancer therapy, Expert Rev. Anticancer Ther. 18 (2018) 1249-1270.

[6] P.M. Fischer, Approved and Experimental Small-Molecule Oncology Kinase Inhibitor Drugs: A Mid-2016 Overview, Med. Res. Rev. 37 (2017) 314-367.

[7] P.A. Futreal, L. Coin, M. Marshall, T. Down, T. Hubbard, R. Wooster, N. Rahman, M.R. Stratton, A census of human cancer genes, Nat. Rev. Cancer, 4 (2004) 177-183.

[8] S. Soverini, R. Bassan, T. Lion, Oncology, Treatment and monitoring of Philadelphia chromosome-positive leukemia patients: recent advances and remaining challenges, J. Hematol. Oncol. 12 (2019) 39.

[9] A. Quintás-Cardama, J. Cortes, Molecular biology of bcr-abl1–positive chronic myeloid leukemia, Blood, 113 (2009) 1619-1630.

[10] A. Desogus, S. Schenone, C. Brullo, C. Tintori, F. Musumeci, Bcr-Abl tyrosine kinase inhibitors: a patent review, Expert Opin. Ther. Pat. 25 (2015) 397-412.

[11] B.J. Druker, S. Tamura, E. Buchdunger, S. Ohno, G.M. Segal, S. Fanning, J. Zimmermann, N.B. Lydon, Effects of a selective inhibitor of the Abl tyrosine kinase on the growth of Bcr–Abl positive cells, Nat. Med. 2 (1996) 561-566.

[12] E. Jabbour, H. Kantarjian, J. Cortes, Use of Second- and Third-Generation Tyrosine Kinase Inhibitors in the Treatment of Chronic Myeloid Leukemia: An Evolving Treatment Paradigm, Clin. Lymphoma Myeloma Leuk. 15 (2015) 323-334.

[13] F.E. Nicolini, M.J. Mauro, G. Martinelli, D.-W. Kim, S. Soverini, M.C. Müller, A. Hochhaus, J. Cortes, C. Chuah, I.H. Dufva, J.F. Apperley, F. Yagasaki, J.D. Pearson, S. Peter, C. Sanz Rodriguez, C. Preudhomme, F. Giles, J.M. Goldman, W. Zhou, Epidemiologic study on survival of chronic myeloid leukemia and Ph+ acute lymphoblastic leukemia patients with BCR-ABL T315I mutation, Blood, 114 (2009) 5271-5278.

[14] A. Quintás-Cardama, H. Kantarjian, J. Cortes, Flying under the radar: the new wave of BCR–ABL inhibitors, Nat. Rev. Drug Discov. 6 (2007) 834.

[15] A.P. Azevedo, A. Reichert, C. Afonso, M.D. Alberca, P. Tavares, F. Lima, BCR-ABL V280G Mutation, Potential Role in Imatinib Resistance: First Case Report, Clinical Medicine Insights: Oncology, 11 (2017) 1179554917702870.

[16] E. Weisberg, P.W. Manley, S.W. Cowan-Jacob, A. Hochhaus, J.D. Griffin, Second generation inhibitors of BCR-ABL for the treatment of imatinib-resistant chronic myeloid leukaemia, Nat. Rev. Cancer, 7 (2007) 345.

[17] M. Copland, A. Hamilton, L.J. Elrick, J.W. Baird, E.K. Allan, N. Jordanides, M. Barow, J.C. Mountford, T.L. Holyoake, Dasatinib (BMS-354825) targets an earlier progenitor population than imatinib in primary CML but does not eliminate the quiescent fraction, Blood, 107 (2006) 4532-4539.

[18] R.W. Hendriks, S. Yuvaraj, L.P. Kil, Targeting Bruton´s tyrosine kinase in B cell malignancies, Nat. Rev. Cancer, 14 (2014) 219.

[19] R. Küppers, Mechanisms of B-cell lymphoma pathogenesis, Nat. Rev. Cancer, 5 (2005) 251-262.

[20] S. Pal Singh, F. Dammeijer, R.W.J.M.C. Hendriks, Role of Bruton's tyrosine kinase in B cells and malignancies, Mol. Cancer, 17 (2018) 57.

[21] M. Rada, N. Barlev, S. Macip, BTK: a two-faced effector in cancer and tumour suppression, Cell Death Dis. 9 (2018) 1064.

[22] J.A. Burger, Bruton's Tyrosine Kinase (BTK) Inhibitors in Clinical Trials, Curr. Hematol. Malig. Rep. 9 (2014) 44-49.

[23] S. Parmar, K. Patel, J. Pinilla-Ibarz, Ibrutinib (imbruvica): a novel targeted therapy for chronic lymphocytic leukemia, P T, 39 (2014) 483-519.

[24] J. Wu, C. Liu, S.T. Tsui, D. Liu, Oncology, Second-generation inhibitors of Bruton tyrosine kinase, J. Hematol. Oncol. 9 (2016) 80.

[25] S.M. Farag, D. Newton, G. Doody, L.A. Mahmoud, M.I. Fouda, D.M. El Ghannam, P. Hillmen, Molecular Mechanisms of Ibrutinib Resistance: Defining a Logical Approach to Improving Targeted Therapy in CLL, Blood, 128 (2016) 2046-2046.

[26] D. Mertens, S. Stilgenbauer, Ibrutinib-resistant CLL: unwanted and unwonted!, Blood, 129 (2017) 1407-1409.

[27] E. Ratzon, I. Bloch, M. Nicola, E. Cohen, N. Ruimi, N. Dotan, M. Landau, M. Gal, A Small Molecule Inhibitor of Bruton's Tyrosine Kinase Involved in B-Cell Signaling, ACS Omega, 2 (2017) 4398-4410.

[28] S. Sharma, J. Singh, R. Ojha, H. Singh, M. Kaur, P.M.S. Bedi, K. Nepali, Design strategies, structure activity relationship and mechanistic insights for purines as kinase inhibitors, Eur. J. Med. Chem. 112 (2016) 298-346.

[29] Y. Wang, W.C. Shakespeare, W.-S. Huang, R. Sundaramoorthi, S. Lentini, S. Das, S. Liu, G. Banda, D. Wen, X. Zhu, Q. Xu, J. Keats, F. Wang, S. Wardwell, Y. Ning, J.T. Snodgrass, M.I. Broudy, K. Russian, D. Dalgarno, T. Clackson, T.K. Sawyer, Novel N9-arenethenyl purines as potent dual Src/Abl tyrosine kinase inhibitors, Bioorg. Med. Chem. Lett. 18 (2008) 4907-4912.

[30] Q. Shi, A. Tebben, A.J. Dyckman, H. Li, C. Liu, J. Lin, S. Spergel, J.R. Burke, K.W. McIntyre, G.C. Olini, J. Strnad, N. Surti, J.K. Muckelbauer, C. Chang, Y. An, L. Cheng, Q. Ruan, K. Leftheris, P.H. Carter, J. Tino, G.V. De Lucca, Purine derivatives as potent Bruton's tyrosine kinase (BTK) inhibitors for autoimmune diseases, Bioorg. Med. Chem. Lett. 24 (2014) 2206-2211.

[31] E.A. Sudbeck, X.-P. Liu, R.K. Narla, S. Mahajan, S. Ghosh, C. Mao, F.M. Uckun, Structure-based Design of Specific Inhibitors of Janus Kinase 3 as Apoptosis-inducing Antileukemic Agents, Clin. Cancer Res. 5 (1999) 1569.

[32] Y. Meng, C. Gao, D.K. Clawson, S. Atwell, M. Russell, M. Vieth, B. Roux, Predicting the Conformational Variability of Abl Tyrosine Kinase using Molecular Dynamics Simulations and Markov State Models, J. Chem. Theory Comput. 14 (2018) 2721-2732.

[33] J. Calderon-Arancibia, C. Espinosa-Bustos, A. Canete-Molina, R.A. Tapia, M. Faundez, M.J. Torres, A. Aguirre, M. Paulino, C.O. Salas, Synthesis and pharmacophore modelling of 2,6,9-trisubstituted purine derivatives and their potential role as apoptosis-inducing agents in cancer cell lines, Molecules, 20 (2015) 6808-6826.

[34] M.G. Brasca, N. Amboldi, D. Ballinari, A. Cameron, E. Casale, G. Cervi, M. Colombo, F. Colotta, V. Croci, R. D'Alessio, F. Fiorentini, A. Isacchi, C. Mercurio, W. Moretti, A. Panzeri, W. Pastori, P. Pevarello, F. Quartieri, F. Roletto, G. Traquandi, P. Vianello, A. Vulpetti, M. Ciomei, Identification of N,1,4,4-Tetramethyl-8-{[4-(4-methylpiperazin-1-yl)phenyl]amino}-4,5-dihydro-1H-pyrazolo[4,3-h]quinazoline-3-carboxamide (PHA-848125), a Potent, Orally Available Cyclin Dependent Kinase Inhibitor, J. Med. Chem. 52 (2009) 5152-5163.

[35] L.A. Byers, L. Diao, J. Wang, P. Saintigny, L. Girard, M. Peyton, L. Shen, Y. Fan, U. Giri, P.K. Tumula, M.B. Nilsson, J. Gudikote, H. Tran, R.J.G. Cardnell, D.J. Bearss, S.L. Warner, J.M. Foulks, S.B. Kanner, V. Gandhi, N. Krett, S.T. Rosen, E.S. Kim, R.S. Herbst, G.R. Blumenschein, J.J. Lee, S.M. Lippman, K.K. Ang, G.B. Mills, W.K. Hong, J.N. Weinstein, I.I. Wistuba, K.R. Coombes, J.D. Minna, J.V. Heymach, An Epithelial–Mesenchymal Transition Gene Signature Predicts Resistance to EGFR and PI3K Inhibitors and Identifies Axl as a Therapeutic Target for Overcoming EGFR Inhibitor Resistance, Clin. Cancer Res. 19 (2013) 279.

[36] A. Mollard, S.L. Warner, L.T. Call, M.L. Wade, J.J. Bearss, A. Verma, S. Sharma, H. Vankayalapati, D.J. Bearss, Design, Synthesis, and Biological Evaluation of a Series of Novel AXL Kinase Inhibitors, ACS Med. Chem. Lett. 2 (2011) 907-912.

[37] S. Krajcovicova, M. Soural, Solid-Phase Synthetic Strategies for the Preparation of Purine Derivatives, ACS Comb. Sci. 18 (2016) 371-386.

[38] M.T. Fiorini, C. Abell, Solution-phase synthesis of 2,6,9-trisubstituted purines, Tetrahedron Lett. 39 (1998) 1827-1830.

[39] T. Gucky, E. Reznickova, T. Radosova Muchova, R. Jorda, Z. Klejova, V. Malinkova, K. Berka, V. Bazgier, H. Ajani, M. Lepsik, V. Divoky, V. Krystof, Discovery of N(2)-(4-Amino-cyclohexyl)-9-cyclopentyl- N(6)-(4-morpholin-4-ylmethyl-phenyl)- 9H-purine-2,6-diamine as a Potent FLT3 Kinase Inhibitor for Acute Myeloid Leukemia with FLT3 Mutations, J. Med. Chem. 61 (2018) 3855-3869.

[40] J.S. Tokarski, J.A. Newitt, C.Y.J. Chang, J.D. Cheng, M. Wittekind, S.E. Kiefer, K. Kish, F.Y.F. Lee, R. Borzillerri, L.J. Lombardo, D. Xie, Y. Zhang, H.E. Klei, The Structure of Dasatinib (BMS-354825) Bound to Activated ABL Kinase Domain Elucidates Its Inhibitory Activity against Imatinib-Resistant ABL Mutants, Cancer Res. 66 (2006) 5790-5797.

[41] Y. Lou, X. Han, A. Kuglstatter, R.K. Kondru, Z.K. Sweeney, M. Soth, J. McIntosh, R. Litman, J. Suh, B. Kocer, D. Davis, J. Park, S. Frauchiger, N. Dewdney, H. Zecic, J.P. Taygerly, K. Sarma, J. Hong, R.J. Hill, T. Gabriel, D.M. Goldstein, T.D. Owens, Structure-Based Drug Design of RN486, a Potent and Selective Bruton's Tyrosine Kinase (BTK) Inhibitor, for the Treatment of Rheumatoid Arthritis, J. Med. Chem. 58 (2015) 512-516.

[42] D.M. Hawkins, The Problem of Overfitting, J. Chem. Inf. Comput. Sci. 44 (2004) 1-12.

[43] J.G. Topliss, R.P. Edwards, Chance factors in studies of quantitative structure-activity relationships, J. Med. Chem. 22 (1979) 1238-1244.

[44] E.F. Pettersen, T.D. Goddard, C.C. Huang, G.S. Couch, D.M. Greenblatt, E.C. Meng, T.E. Ferrin, UCSF Chimera—A visualization system for exploratory research and analysis, J. Comput. Chem. 25 (2004) 1605-1612.

[45] M. McGann, FRED Pose Prediction and Virtual Screening Accuracy, J. Chem. Inf. Model. 51 (2011) 578-596.

[46] S. Genheden, U. Ryde, The MM/PBSA and MM/GBSA methods to estimate ligand-binding affinities, Expert Opin. Drug Discov. 10 (2015) 449-461.

Highlights

Design and synthesis of new 2,6,9-trisubstituted purine derivatives.

Compounds **5c** and **5d** were potent inhibitors of both kinases, with IC_{50} values of 40 nM and 0.58/0.66 μM for Abl and Btk, respectively.

Structural requirements for Bcr-Abl and Btk inhibition were analyzed with docking and 3D-QSAR.

5c and **5d** could suppress the proliferation of leukemia and lymphoma cells at low micromolar concentrations *in vitro.*

5c inhibited the downstream signaling of both kinases in the respective cell models.